UDC 550.839 http://doi.org/10.21440/2307-2091-2024-1-33-76

Geo-petrophysical analysis of hydrocarbon in the Douala Campo basin, Cameroon

Bareja YOUMSSI TICHOUE[1*]
Valentina Mikhailovna USOVA[2**]
Sixtus NTEH[1***]
Elena Mikhailovna KOTEL'NIKOVA[2****]

[1]The University of Bamenda, Bamenda, Cameroon
[2]Peoples' Friendship University of Russia (RUDN University), Moscow, Russia

Abstract

The relevance of the work. Well-log analysis and 3D seismic method are combined to evaluate the nature of fluids and reservoir characteristics in the Douala-Campo basin (DC). Scientific research that exhibit the important geologic and geophysical settings of this basin is lacking.

The purpose of the work. The successful investigation of these areas is possible if the stratigraphic and petrophysical properties of the reservoir are properly evaluated.

Research methodology. Extracting facies types from 3D seismic sections is a rapidly evolving discipline that facilitates the development of reservoir prediction models. Therefore, a 25 m x 25 m seismic grid associated with Gamma-Ray log (GR), Neutron (Nphi) log, resistivity log, sonic log, and density (RHOB) log have been performed.

Results and Conclusions. The results highlight the sedimentary environment and facies, porous-permeable clay banks, clay content, porosity, saturation and the nature of the fluids in the reservoir. The petrophysical evaluations indicate potential petroleum reservoirs, mainly sandy-clay with 3.81–29.47% volume, 17.37–27.85% porosity and 27.74–56.02% water saturation. The fluids present in the reservoir is oil, gas and water. This research will encourage hydrocarbon (HC) exploration in the DC Basin by adopting strategies in which seismic stratigraphy combined with well data will be the most likely means of providing drilling targets for more independent operators. The results of this study will serve future prospectors in the neighbouring oil and gas fields of our study area. Significant advances have been made to ensure future exploration success.

***Keywords*:** 3D seismic, Reservoir, Well log, Petrophysical parameters, DC.

Introduction

As a result of the separation of the African and South American tectonic plates, the opening of the South Atlantic (from the Berriasian to the Upper Aptian) began in the early Cretaceous as a gradual diachronic North-South process [1, 2]. Due to a marine incursion, this opening introduced a range of salt basins, giving rise to various basins: Namibia, Benguela and Cuenza (Angola), Douala-Campo (DC), Namibia, Rio Del Rey (RDR) (Cameroon), and Rio Muni (Gabon/Equatorial Guinea) [3]. The volcanic line marks the edge between the two coastal basins for Cameroon. The RDR basin is the southern extension of the Niger Delta, while the DC basin develops along the Gulf of Guinea [4]. Cameroon seeks to increase its production in hydrocarbon by promoting several oil field block in the Douala-Campo basin (DC) basin. The exploration of new hydrocarbon reserves is known to be expensive, so it is necessary to use low-cost methods to locate and quantify these reservoirs within the limitations of geological models. The derivation of stratigraphic insights from seismic data has its origins in the early 1970's with the advent of improved 2D seismic data. The discipline of seismic stratigraphy traces its roots to the landmark publication of AAPG Memoir 26, which summarized the work of Peter Vail and his colleagues at Exxon Production Research Company [5]. The seismic expression of stratigraphic features in a 3D seismic cube depends on which way the data volume is being viewed; vertical transect or horizontal map view [6].

Well-logging data can accurately detect reservoir fluid volume and composition, if interpreted correctly and ideally calibrated to core data [7–13]. Gamma logs are used to reveal lithology such as shale beds. Similarly, gamma logs are used to identify other lithology such as dolomites and limestone when available from core data. Resistivity logging is used to discern water and hydrocarbons in reservoir rock interstices. It can be used to determine the oil-water contact and the true resistivity of the formation [14]. Hydrocarbons are encountered in ecological traps,

✉youmssi@mail.ru
** usova-vm@rudn.ru
https://orcid.org/0000-0002-0023-5913
***ntehsixtus@gmail.com
****kotelnikova-em@rudn.ru
https://orcid.org/0000-0001-8909-8953

which may be stratigraphic, structural, or a combination of both. Most traps in the Niger Delta, according to Doust and Omatsola (1990) are structural [15]. Oil drilling is an expensive undertaking, especially as supplies of hydrocarbons decline. Undiscovered deposits are located in intricate geological environments, so capitalizing on new developments is essential [16]. Keys to quantifying producible hydrocarbons are reservoir characteristics, in particular the water saturation thickness, reservoir, porosity and zone extent (Schlumberger, 1998). Information on these parameters is relevant and serve as input data for the volumetric analysis of the reservoir, i.e. the volume of hydrocarbons in place [17]. Many oil wells drilled in the DKC basin based on 2D seismic data have failed due to poor reservoir quality, and according to the drilling completion reports, these wells may not have been optimally positioned with respect to the reservoir target. This study aims to determine the nature of the hydrocarbons and to characterize the reservoirs in the study area. This is achieved by identifying the nature of the fluids, the potential reservoirs and by estimating petrophysical parameters from well logs. This research will encourage hydrocarbon (HC) exploration in the DC Basin by adopting strategies in which seismic stratigraphy combined with well data will be the most likely means of providing drilling targets for more independent operators [18–20]. The results of this study will serve future prospectors on the neighbouring oil and gas fields of our study area. Significant advances have been made to ensure future exploration success in the DKC basin of Cameroon.

Location and geology of the study area

The DKC basin is located between 9°04'–10°04' East longitude and 2°18'–4°32' North latitude (Fig. 1). The DKC basin encompasses an area of 19,000 km^2. The DKC Basin is divided into two sub-basins, one in the south, the Kribi-Campo Sub-basin, and one in the north, the Douala Subbasin [21]. Hydrocarbon exploration in the DKC basin began in the fifties at the onshore portion. The offshore part of this basin was explored in the 1960s and was primarily concentrated in the shallow water Kribi-Campo sub-basin, targeting the inclined cretaceous fault provinces that extend to onshore where oil derived from the Cretaceous formation is currently produced [21]. The Douala basin geology history begins in the Lower Cretaceous with the discontinuity that separates Africa and South American continents. The formation of the first deposits of the lower Mundeck formation begins the filling of the basin during this initial rift phase [22, 23]. This filling starts with the Aptian in the Douala sub-basin and the Barremian in the Kribi-Campo sub-basin [23, 24]. Lower Mundeck continental deposits include sandstone (base sandstone), dark gray shale clay, organic-rich marl, thin limestone beds, and conglomerate [25]. Toward the end of the Aptian, during a transition period, the first marine incursions produced a salifer series that spread from Cameroon to Angola [26]. There are three separation intervals from the Albian to the current, during which a passive margin was formed by the accumulation of sedimentary deposits in discrepancy, separated by cuts caused by orogenesis phases [25, 27].

The significant marine transgression of the Drift I phase in Albien results in the formation of the upper Mundeck layers, which are composed of sandstone, argillite, organic clay, and carbonate past. This succession usually ends with the " Cenomanian discordance", which is the result of the start of

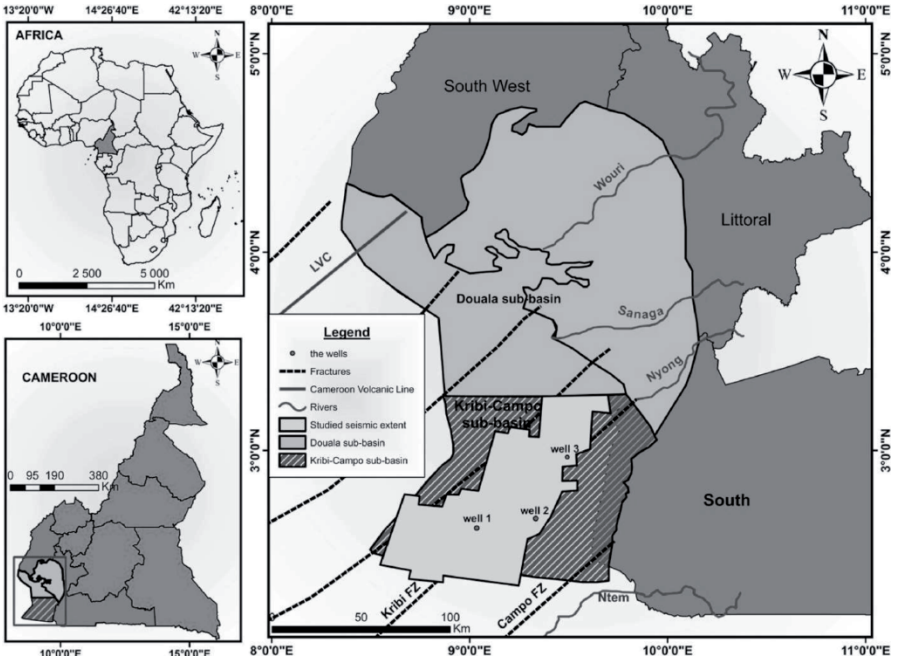

Figure 1. Location map indication the seismic grid extent and well log position

Рисунок 1. Карта местоположения с указанием протяженности сейсмической сетки и положения каротажных диаграмм

a regression that continues to the Turonian [28]. The Drift II phase, which is linked to the Santonian's Tectonian episode, is separated from Phase I (Drift I) by a discontinuity caused by this event. Following the latter, the formation of Logbadjek, made of micro-conglomerate, sand, middle sandstone to rude and rare limestone and clay intercalates, already begins in the Santonian and continues at the lower campanien. The thick formation of logbaba formed of sediments sailors of deep-sea water follows in this one, in the upper campanien and the Maastrichthen. These sediments are made up of fossilized argillitis with sand levels and sandstone [4, 22]. The Mastrichtic Terminal and Danian gap highlight the Cretaceous Passage-Tertiary in all Western African basins. Tertiary sedimentation in the Douala Basin begins with the filing of NKAPA training by simple subsidence of the passive margin. This lower Paleocene-Eocene formation is composed of silt, sand lentils, dolomite, clay literate, argillite, and fine friable sandstone with coarse [4, 29].

During the Eocene, sedimentation is abruptly halted by a major episode of medium tertiary lifting, resulting in the great stratigraphic gap of lower higher-oligocene Eocene. The Songlaba formation, oligoMiocene, produces a subsidence and beginner at the same time as the Drift III phase at the end of the Oligocene [27]; it is characterized by marls, sandstones, silts, and clays with interstracted sand lentils and occasionally shell limestones. The Cenozoic series concludes with the formations of Matanda (Pliocene) and Wouri (Pleistocene) made of fine sand in rough, clay, and volcanic tufa after a final stratigraphic gap at the end of the Miocene.

Seven formations (Fig. 2) were described in the Douala sub-basin based on the previous works [3, 22–24, 27, 30]. Mundeck formation is the oldest to the most recent. The term "Mundeck Formation" refers to the lower Cretaceous Age Section of the Sismic discordance [31]. This formation is the oldest, dated C´enomanian [23, 31], and it is located in the precarambrian base discrepancy. It is located in the Moungo Valley, near Mundeck, in the northern part of the Douala sub-basin. Mundeck is made up of continental and fluvio-deltaic deposits with some marine facies intercalates [23]. It is a thick layer composed of base elements, medium to coarse sandstone, micaceous fine sandstone, carbonneous and carbonate, black shale micas, argilites, limestones, and marls [4, 32].

The logbadjeck formation is in concordance or discordance with the Mundeck formation, as a result of Turonian regression and the erosion of the base and basic sandstone. It is made up of microconglomerates, sands, rough medium sandstones, fossiliferous limestone and sandy clay intercalations, sandstone, and marn-limestone intercalates [4]. It has been eroded to the east due to Turonian flexuration. The formation of logbadjeck from the outcrop is well represented in the Moungo Valley, where it represents deposits of the basin's external platform. Logbajeck's formation is dated as Cenomanian and Campanian [4, 33, 34]. Sedimentation is primarily fluvio-deltaic at the base. The Formation of logbaba is a thick sedimentary layer dominated by argillites, with a summit characterized by an upper Cretaceous discrepancy [4].

The logbaba formation sediments are marine, deposited in deep water with rapid landfill, a feature of the development of West African basins with deepwater argilites. This field is made up of sandstones, sands, and fossilized argillitis [4, 22]; it is Campanien-Maastrichthen dated [4, 31].

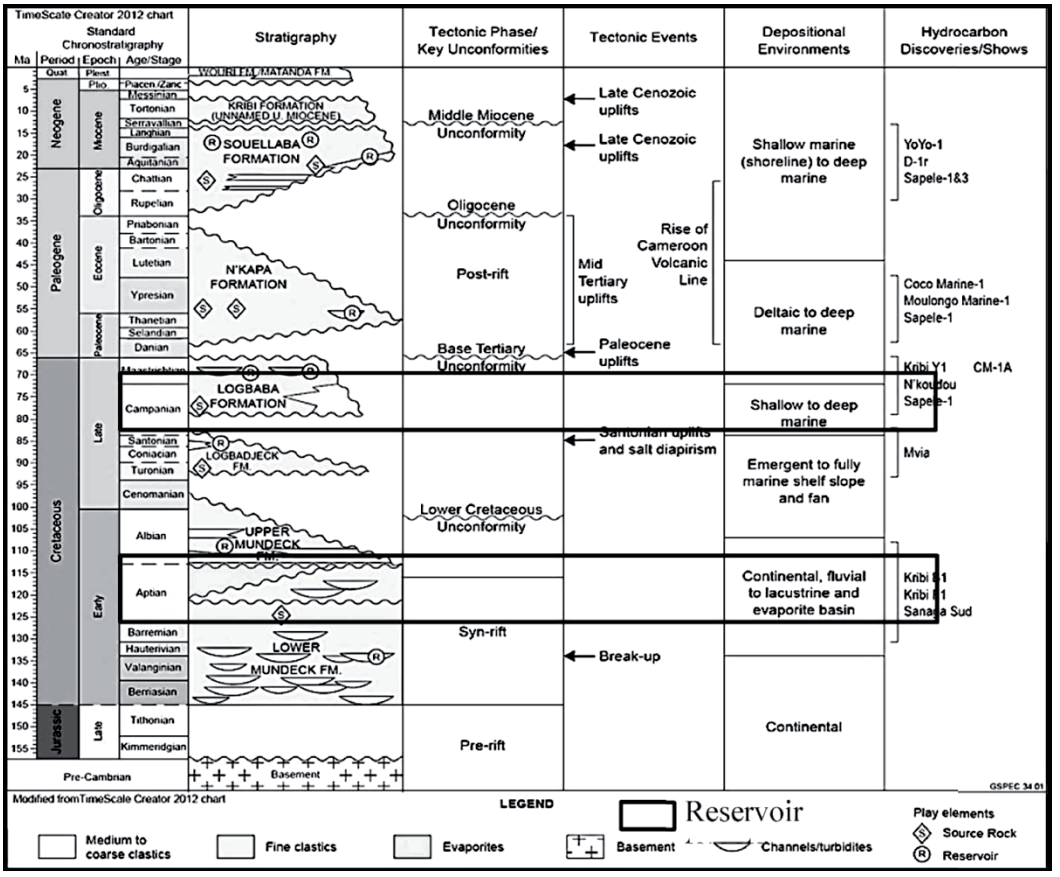

Figure 2. Lithostratigraphy of DC basin [33]
Рисунок 2. Литостратиграфия бассейна ДК [33]

The Nkapa formation is underlain by Cenozoic unconformities, indicating Tertiary sedimentation by passive margin subsidence. Its formation comes to an end abruptly in the Middle Eocene after a major episode of uplift and erosion of the African margin. The Nkapa Formation, which separates from the Logbaba Formation to the east and southeast of the sub-basin, is heavily eroded. It can be seen in the Moungo Valley outside the outcrop [35]. It is composed of shales, calcareous clays, arkosic sandstones, fine friable sandstones with crusts, silts, sands, and dolomitic lenses and is of Lower Paleocene age [4, 29]. Logar (1983) describes the deposit context as a coexistence of continental and marine environments. From a coastal clay-silt environment, the environment evolves to the south towards a more marine environment marked by turbidite sandy deposits [4].

The formation of Songelaba is the result of subsidence and resumption of sedimentation following the important phase of lifting and erosion responsible for the large stratigraphic gap of the higher Eocene [21, 23, 35]. Because of the erosion of upper ecene and lower oligocene sediments, the formation of Songelaba is dated higher-miocene lower Oligocene [23, 36]. It is distinguished by marls and lentils of interstracted sands in intercalation [4, 22] and, on rare occasions, by shell limestone [31]. Clays cover the transgressive sandstones and silts that dominate the lower part. Matanda (Superior-Pliocene Miocene) formation is dominated by interstratified deltaic facies and volcanic tuffs [4, 22]. These are coarse sands that begin at the bottom and end at the top, alternating with pockets of clays that are occasionally intersected with basalttes [37].

Matanda formation dumped in Tiko and the Douala basin's coastal area.

The Wouri (Pliocene-Pleistocene) formation is distinguished by coarse gravel and gravel with clay matrix [4]. There is often evidence of lava and volcanic tufas. Wouri sediments are the result of estuarine sedimentation at the mouths of the Wouri and Dibamba rivers.

Materials and methods

The evaluation of the oil potential of the southern part of the DKC basin is carried out through the analysis of conventional 3D seismic and well log data. The 3D seismic database investigated is located in offshore part. A 25 m × 25 m grid-oriented NS-EW was generated and two vertical wells namely P1 and P2 have been used for well log recording. Seismic data analysis involved coordinate conversion, data loading, well to seismic tie using synthetic seismogram, horizon and facies illustration, amplitude map generation [38].

Seismic calibration is done using two logs (sonic, density) and checkshots. The sonic is first calibrated, then the multiplication of the sonic and the density will generate the acoustic impedance and the coefficient of reflectivity. This will then be convoluted to an appropriate wavelet extracted from the seismic to generate the synthetic seismogram. It will subsequently make to better find the time-depth correspondences or to better correlate.

After seismic calibration, therefore come the seismic interpretation. The method used is manual picking and semi-automatic tracking [39]. It is a completely manual operation which aims to point at an object of interest using the desktop mouse and the tracking is both manual and software assisted. At each point, the software researches similar information (polarity, amplitude and similar frequency) between the different points, respecting the principles of stratigraphy. The different points will thus be joined to allow obtaining a horizon at the end of the process. Then the amplitude map was generated.

The main logs used for this study are the Gamma-Ray log (*GR*) which allowed us to delineate the porous-permeable clay banks and estimate the clay content in each reservoir; the Neutron log (Nphi) in combination with the density log (RHOB), this log allowed us to determine the porosity of the formations and to reconstruct the lithology crossed by each well; the density log (RHOB) allow us to identify the fluids in the reservoirs and to locate the gas/oil and oil/water contacts in comparison with the neutron and resistivity logs; and resistivity logs allowed us to calculate saturations and determine the nature of the fluids.

The petrophysical assessment can be classified into two successive stages: Qualitative assessment: Quick look analysis and Quantitative evaluation (single-plot analysis).

This method of rapid interpretation of logs developed by Serra (1979) allows a qualitative analysis, which requires practically no calculation, mainly using the comparison of logs with each other by superposition. This evaluation method is subdivided into two stages [40]:

– Identification of lithology, the method used is the cutting of the logs into electrofacies zone by highlighting the different polarities and allows to delimit the possible zones of being reservoirs; to do this we look at the positions of the neutron log (Nphi) and the density log (RHOB);

– Determination of porosity and type of hydrocarbon, a certain number of conditions must be fulfilled for the determination of these parameters.

The single-plot analysis it is an analysis that provides information on the petrophysical parameters (shale volume, porosity, saturation, permeability, etc.). In order to interpret measurements quantitatively, the electrical resistivities measured depend on the natural geological conditions and the action of the drilling fluids used. It is important to bring the various resistivities to the temperature of the formation considered, for this it is necessary successively to determine the petrophysical parameters such as: the volume of shale (V_{sh}) by using Eq. (1); the effective porosity (PhiE) and water saturation (S_w).

Table 1. Petrophysical parameters of reservoir in well P1
Таблица 1. Петрофизические параметры пласта в скважине P1

Reservoirs	Depth, m, TVD	Thickness, m	V_{sh}, %	PhiE, %	S_w, %	Lithology	Natural fluids
R1	3831–3945	114	15.3	24.85	53.98	Sandy shale	Gas
R2	4072–4105	33	5.04	19.06	55.91	Sand	Oil
R3	4235–4305	70	7.87	18.97	54.91	Sand	Oil
R4	4323–4431	108	3.81	20.81	54.03	Sand	Oil
R5	4463–4549	86	7.36	18.05	56.02	Sand	Oil

To achieve the objectives, we carried out the following steps: (*i*) Sampling of the number of electrofacies, (*ii*) Identify the roofs and bases of the reservoirs selected, (*iii*) Then proceed to the calculation of the petrophysical parameters, (*iv*) Determination of the volume of shale from the *GR* [41]. Prior to these tasks, the baseline of the sand and shale needs to be calibrated taking the average of the log *GR*

$$V_{\text{sh}} = I_{\text{GR}} = \frac{GR_{\text{read}} - GR_{\text{min}}}{GR_{\text{max}} - GR_{\text{min}}}, \quad (1)$$

where GR_{read} is the *GR* value of the bank read directly from the log; GR_{min} is the minimum *GR* value of the same bank; GR_{max} is the maximum *GR* value of the same bank, all of them in the API unit. I_{GR} is the Gamma ray radiation index and V_{sh} is the Volume of shale;

– Determination of the porosity: Log Rhob calibration: The log Rhob must be calibrated according to the shale peak and then calculate the effective porosity (PhiE) using the standard formula [42]. The porosity density is obtained from Wyllie's Eq. (2)

$$\varnothing_D = \frac{\rho_b - \rho_{ma}}{\rho_f - \rho_{ma}}, \quad (2)$$

where $\varnothing_D$ is the overall density read opposite the given study level in, g/cm^3; $\rho_b, \rho_f, \rho_{ma}$ are the density of the matrix, the fluid density and the porosity given by density tools respectively.

Alongside this density porosity, the porosity is determined by the "Quick look" method, which combines neutron and density logs porosity $(\varnothing_N, \varnothing_D)$. The total $\varnothing_T$ and effective porosity $\varnothing_e$ are plotted by the following Eq. (3) and (4):

$$\varnothing_T = \frac{\varnothing_N - \varnothing_D}{2}, \quad (3)$$

and

$$\varnothing_e = \varnothing_T (1 - V_{sh}). \quad (4)$$

Neutron log calibration: this involves bringing the log neutron back to the shale peak and reading the corresponding value;

– Determination of water saturation:

Prior to this, we must first configure the calculation formula, the one used in our work is "Dual Water", this is a formula developed by the Americans [43] and it turns out to be proportional to our environment (sandy shale). Next, you have to calibrate the density and the volume of shale previously calculated from the GR, and finally determine the matrix parameters (*a*, *n* and *m*) used in the Archie Eq. (5).

$$\frac{1}{R_t} = \frac{\varnothing_T^m S_{wT}^n}{aR_w}\left(1 + \frac{BQV_n}{S_{wT}}\right), \quad (5)$$

with $QV_n = \frac{V_{sh}\varnothing_{sh}}{\varnothing_T}$; S_{wT} – Total water saturation; V_{sh} – Volume of clay; $\varnothing_{sh}$ – Clay porosity; *a* – Formation factor; *n* – Saturation exponent, which can vary between 1.2–2.2; *m* – Cementation factor.

Due to the water saturation, S_w, it will be possible to determine the hydrocarbon saturation in the virgin zone S_{hc} with the following Eq. (6):

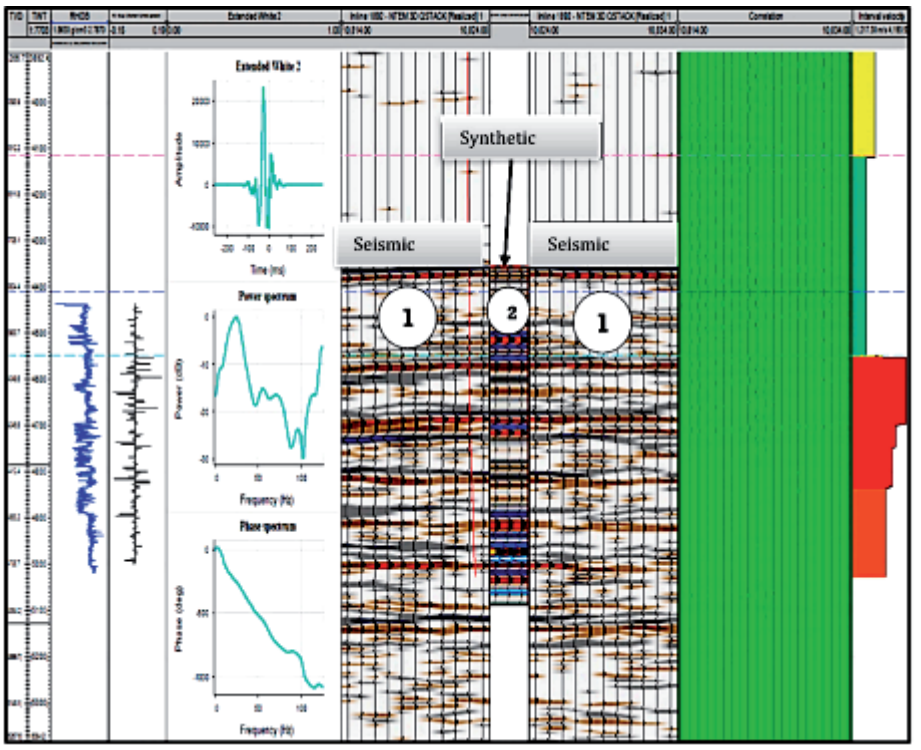

Figure 3. Synthetic seismogram generated by the checkshot and sonic log data in well P1

Рисунок 3. Синтетическая сейсмограмма, полученная по данным контрольного и акустического каротажа в скважине P1

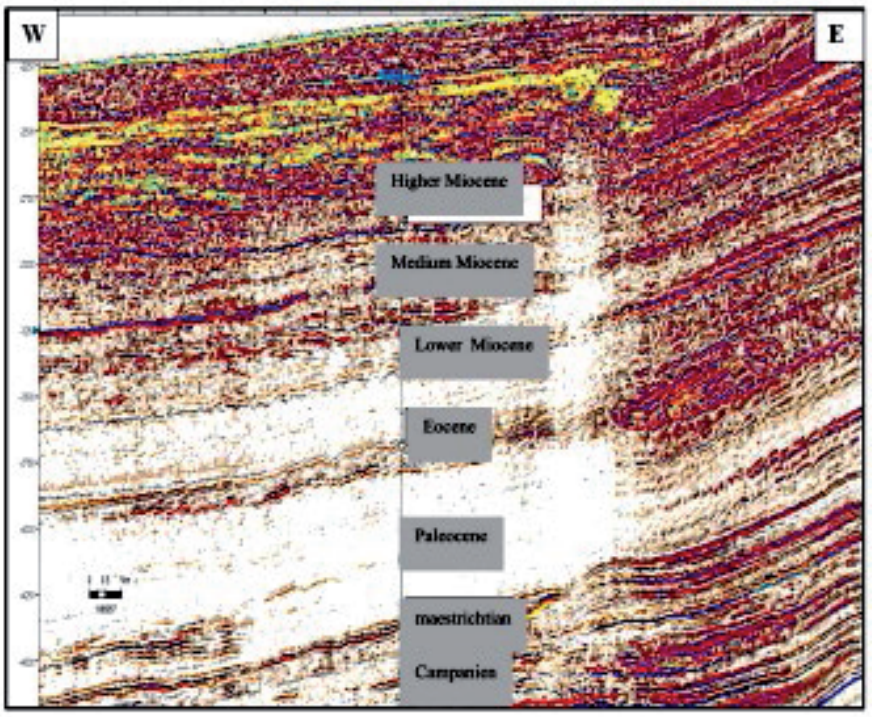

Figure 4. Visualisation of well on the seismic profile
Рисунок 4. Визуализация скважины на сейсмическом профиле

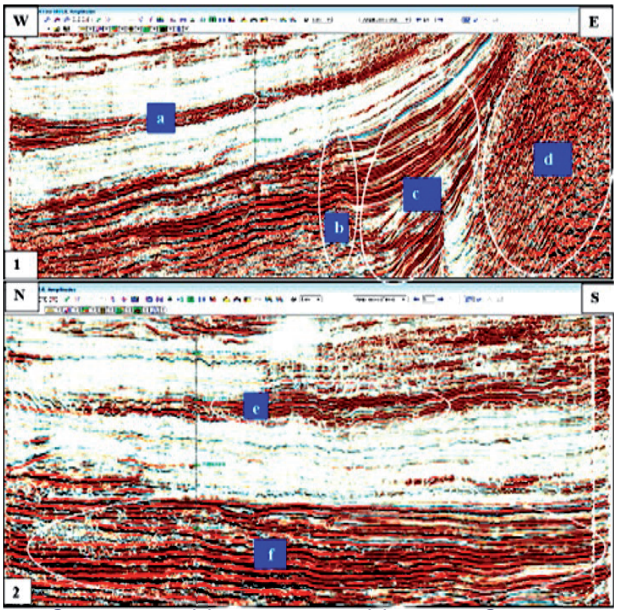

Figure 5. Inline (*1*) and crossline (*2*) indicating facies
Рисунок 5. Прямая (*1*) и перекрестная линия (*2*) с указанием фаций

$$S_{hc} = 1 - S_w; \quad (6)$$

– Nature of fluids determination.

It is noted that, in the oil-bearing reservoir, *GR* and Density-Neutron all deflect to the left. Only resistivity deflects to the right. *GR* reads lower due to lower radioactivity of Th, K and U. Resistivity responds to non-conducive hydrocarbon, giving higher resistivity. Density-Neutron reads higher porosity in reservoir.

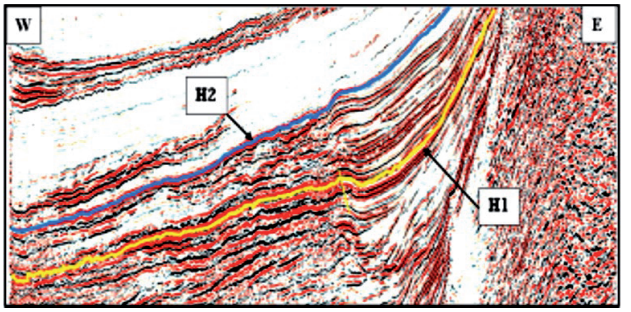

Figure 6. Seismic profile showing the interpreted horizons (H1 and H2)
Рисунок 6. Сейсмический профиль, показывающий интерпретированные горизонты (H1 и H2)

In the gas reservoir, *GR* deflects to the left; Resistivity, right; Density left; and Neutron, right. *GR* reads lower due to lower radioactivity of Th, K and U. Resistivity responds to non-conducive hydrocarbon, giving higher resistivity. Density gives lower bulk density due to lower gas density. Neutron reads low apparent low porosity in gas zone due to lower neutron-hydrogen interactions in gas as compared to neutronhydrogen interactions in water. The use of petrophysical cutoffs for net pay demarcation are as follow: $Gr_{cutoff} = < 0.45$; $PhiE_{cutoff} => 0.1$; $S_{w\,cutoff} = 0.70$.

Results and discussion

1. Seismic well tie result

Fig. 3 above shows the synthetic seismogram generated by the check shoot and sonic log data in well P1. The numbers represent the seismic traces. In 1, we observe the original seismic traces obtained after processing the signals; in 2, it is a synthetic trace generated after calibration. This seismogram allowed us to set the reflectors in the depth range where the logs were recorded. The correlation coefficient between seismic

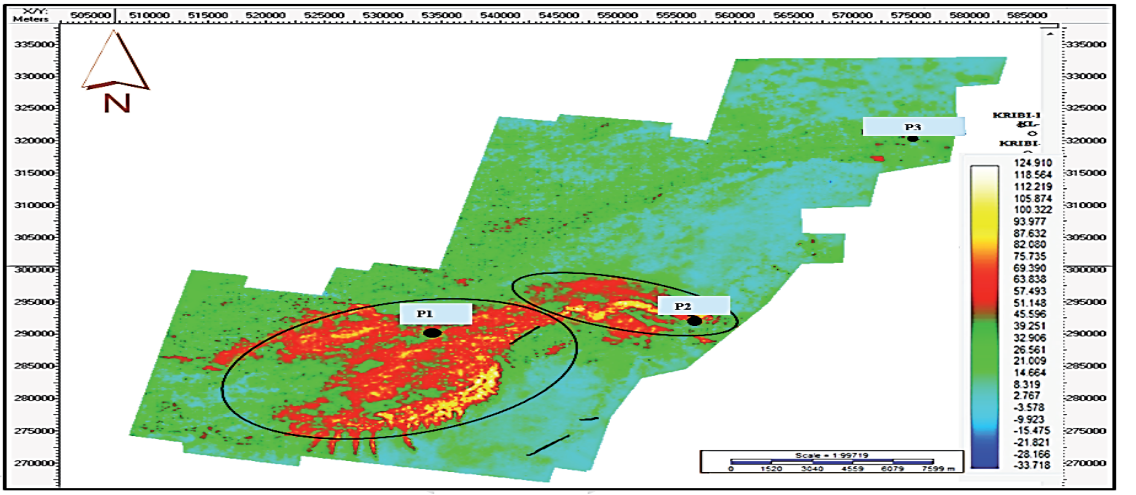

Figure 7. Amplitude (ms) map of the H1 horizon, indicating potential sand accumulation in the areas of high amplitude
Рисунок 7. Карта амплитуды (мс) горизонта H1, показывающая потенциальное скопление песка в областях высокой амплитуды

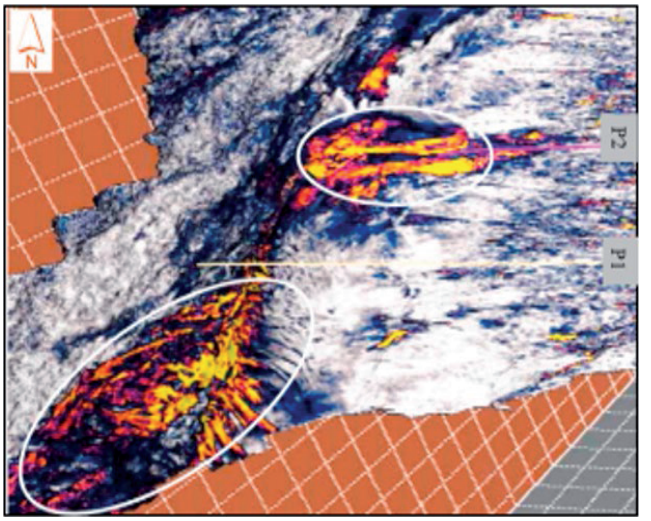

Figure 8. RMS amplitude map (H1) generated on 3D coherence attribute
Рисунок 8. Карта среднеквадратичных амплитуд (H1), созданная на основе трехмерного атрибута когерентности

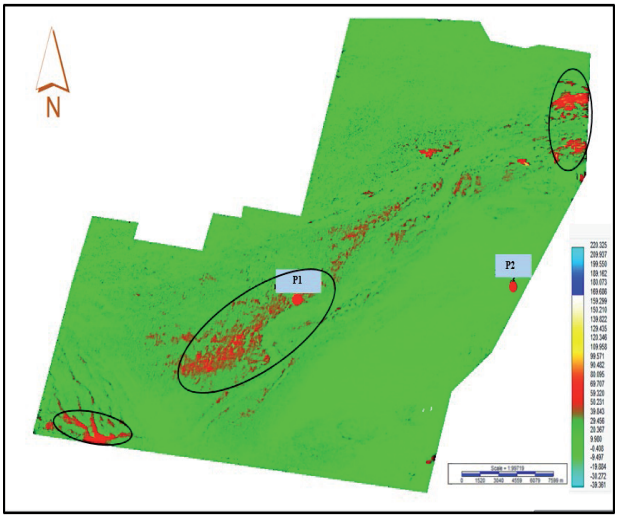

Figure 9. Amplitude (ms) map of the H2 horizon, indicating potential sand accumulation in the areas of high amplitude
Рисунок 9. Карта амплитуд (мс) горизонта H2, указывающая на возможное скопление песка в областях повышенного содержания песка

trace and synthetic trace at the point of intersection obtained at the end of this setting is greater than 0.65, i. e. 65%, the setting of the seismic horizons in time using the data from the P1 well was a success. However, we can note small differences between the amplitudes observed on the surface seismic and synthetic trace. This difference is explained by the choice of amplitude compensation laws used for the two types of data. For this purpose, we can visualize the well on our seismic profile converted to depth (Fig. 4).

2. Seismic interpretation profiles

In the inline profile, we observe four facies represented by the letters a, b, c and d (Fig. 5). The discontinuous facies (a): which are linked to small systems of slightly spaced normal faults, known as "polygonal fault systems". Polygonal faults have been observed along the West African margin, off Angola [44] and in Namibia. They can also be seen on the Crossline profile represented by the letter (e); The monoclinal facies (b): are generally linked to deep water channels controlled by high turbidity currents. The individual mounds are characterized by a continuous convex shape from low to high amplitude and aggressive reflections; The facies in the hollow filling of the channels (c): are almost present over the entire Inline profile with slightly varying depths. The presence of these channels can be explained by the first marine incursions into open space by the first drift phase following the initial rift phase and during which the first oceanic crust formed; The chaotic facies (a): are mainly present at the eastern extension of the basin and can result from more or less coarse and heterogeneous inputs deposited in the sea level bed and at the end of the ascent. Moreover, when these are in depth, they can reflect poor data quality.

In crossline profile, we observe two facies represented by the letters (e) and (f) (Fig. 5):

The discontinuous (e) facies and the parallel (f) facies, which present reflectors with high amplitude and good lateral continuity and high frequency. These facies reflect a sedimentary environment of moderate energy.

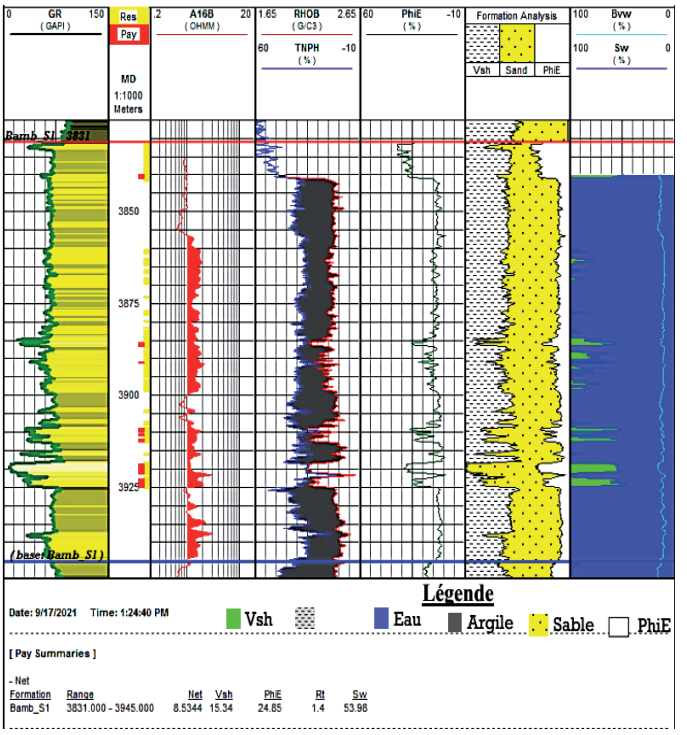

Figure 10. The litho-saturation plots of reservoir 1 of well P1 showing the negative separation between neutron and density logs and could indicate the presence of gas

Рисунок 10. Графики литонасыщенности пласта 1 скважины P1, показывающие отрицательное разделение между нейтронным каротажем и каротажем плотности, могут указывать на присутствие газа

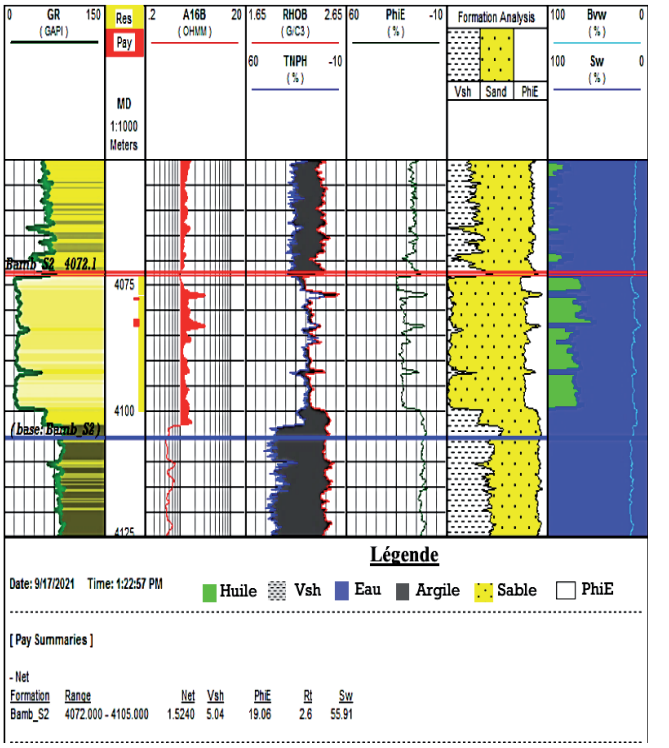

Figure 11. The litho-saturation plots of reservoir 2 of well P1 showing more crossed behaviour between neutron-density logs which could indicate the presence of oil

Рисунок 11. Графики литонасыщенности пласта 2 скважины P1, демонстрирующие более перекрестное поведение между данными нейтронно-плотностного каротажа, что может указывать на наличие нефти

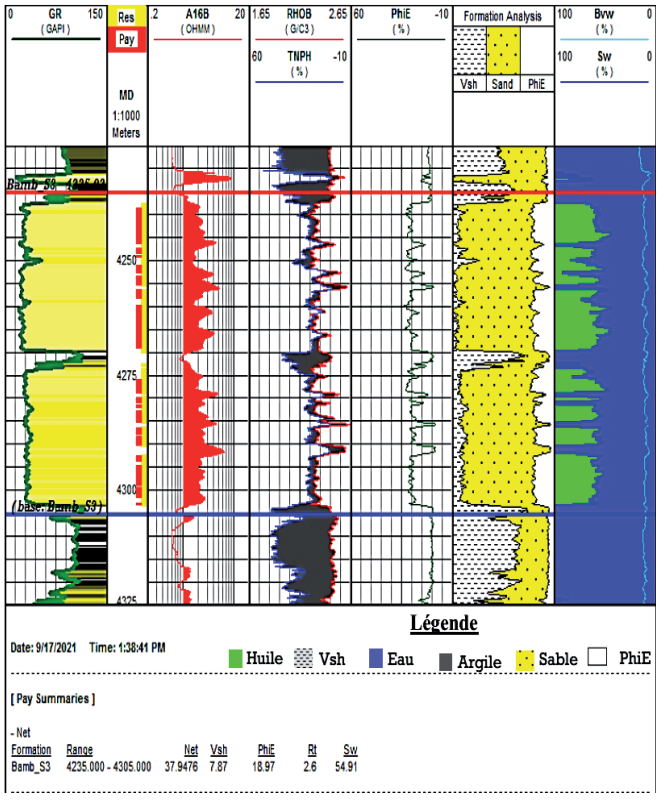

Figure 12. The litho-saturation plots of reservoir 3 of well P1

Рисунок 12. Графики литонасыщения пласта 3 скважины P1

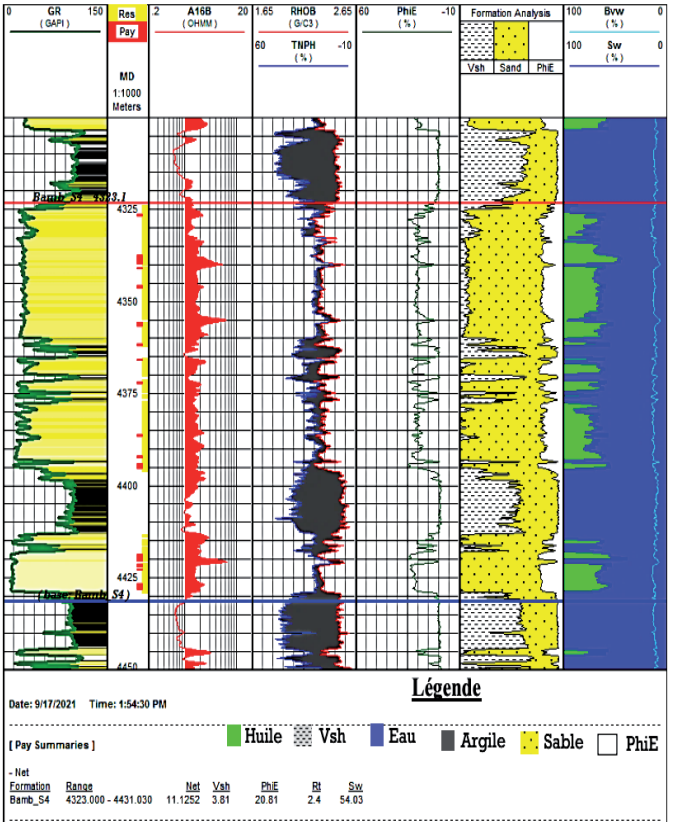

Figure 13. The litho-saturation plots of reservoir 4 of well P1

Рисунок 13. Графики литонасыщения пласта 4 скважины P1

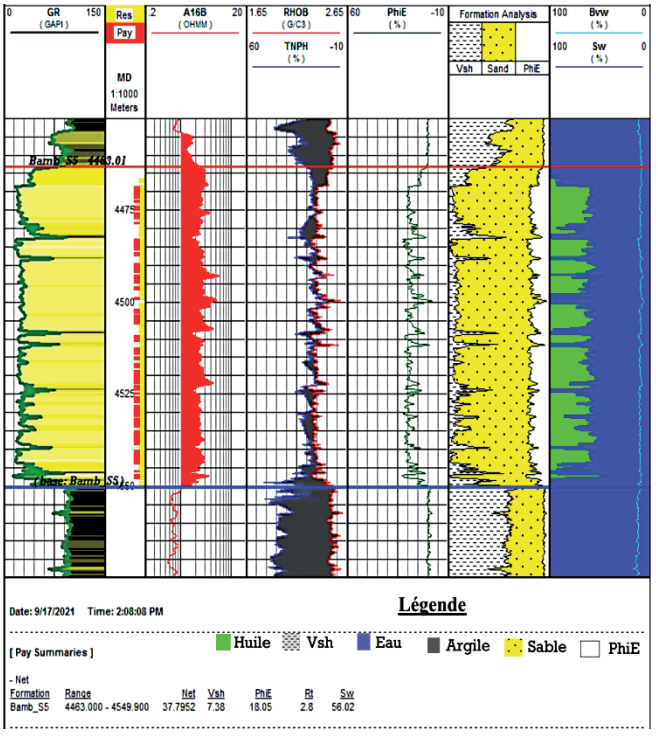

Figure 14. The litho-saturation plots of reservoir 5 of well P1
Рисунок 14. Графики литонасыщения пласта 5 скважины P1

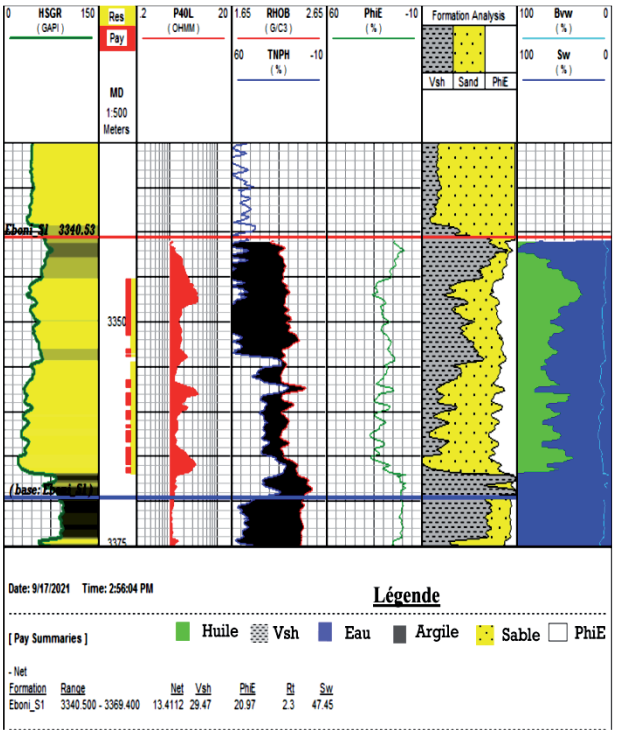

Figure 15. The litho-saturation plots of reservoir 1 of well 2
Рисунок 15. Графики литонасыщенности пласта 1 скважины 2

3. Structural model interpretation

Fig. 6 presents the results of the seismic interpretation (tracking or picking) of the horizons H1 and H2, and the faults with a step of 20 along the seismic volume to retrace the succession and the continuity of the sedimentary deposits in this basin.

Horizon H1: the oldest, it is represented on the profile by a yellow coloring (Fig. 6). This horizon is dated to the Lower Cretaceous, more precisely to the Aptian. It has a high amplitude to medium amplitude reflector along the W-E direction. A steep slope is also following the West direction.

Horizon H2: the most recent and is represented on the profile by a blue coloring (Fig. 6). This horizon is dated to the Upper Cretaceous, more precisely to the Campanian. It has a high amplitude reflector.

In terms of faults, the DKC basin does not have enough faults, however we have spotted three on the H1 horizon. These faults have almost a uniform NE-SW direction and are normal in nature.

4. Amplitude map interpretation

The amplitude maps of the two horizons above show zones with strong contrasts of amplitudes (circled zones) targeted by the two existing boreholes. These zones are marked by red and yellow colors with black outline (Figs. 7–9).

Upon analysis of said maps and the regional geological context in this area of the DKC basin, more precisely in the southern part, the sediments mainly come from the continental shelf westward and were deposited in the seabed by a phenomenon of progradation. Towards the southern end of the basin, we note the presence of a channel visible on both horizons, justified by the first marine incursions into the open space by the first phase of drift following the initial rift phase and during which the first oceanic crust is formed.

This channel therefore favoured the deposition and piling of sediments in this area. Two main directions of sediment deposition, to the east of the basin, the deposits of pure sands deposited along the channels also visible on the H1 and H2 horizons. In view of these results, it clearly appears that the Aptian (H1 horizon) and Campanian (H2 horizon) formations constitute areas of interest in view of their prospectively.

5. Petrophysical interpretation

The high-amplitude areas of interest identified after mapping the H1 and H2 horizons shown in figs. 7, 9, constitute potential sand accumulation (therefore reservoirs). In view of an active petroleum system in the DKC basin, these potential reservoirs could be loaded with hydrocarbons.

Five (05) zone have been identified, after evaluation of the physical parameters. The following results are obtained: according to well logs of location P1 given in figs. 10–14, the porosity (neutron-density) logs of the retained reservoir shows less cross-behaviour in reservoir 1 (Fig. 10), which could associated to gas, and perfect cross-behaviour (Figs. 11–14) in reservoirs 2 to 5, which is a typical indicator of the presence of the oil in these reservoirs.

A considerable increase in resistivity logs can show that the fluids of the formations crossed are permeable and porous. In addition, the effective porosity logs (PhiE) obtained confirm the two hypotheses.

Table 1 shows the synthesis of the petrophysical parameters obtained after evaluation in the reservoir 1. The depth is the True Vertical Depth (TVD).

In Well P2, three (03) reservoirs (Figs. 15–17) were identified, after evaluation of the petrophysical parameters, the following results are obtained:

The logs from the P2 well show less crossed behaviour (negative separation between neutron and density curves)

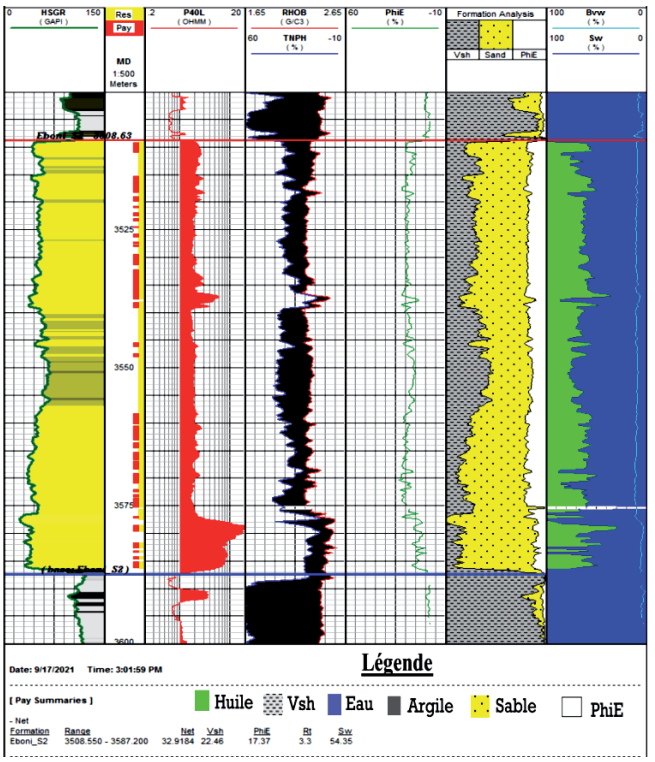

Figure 16. The litho-saturation plots of reservoir 2 of well 2
Рисунок 16. Графики литонасыщения пласта 2 скважины 2

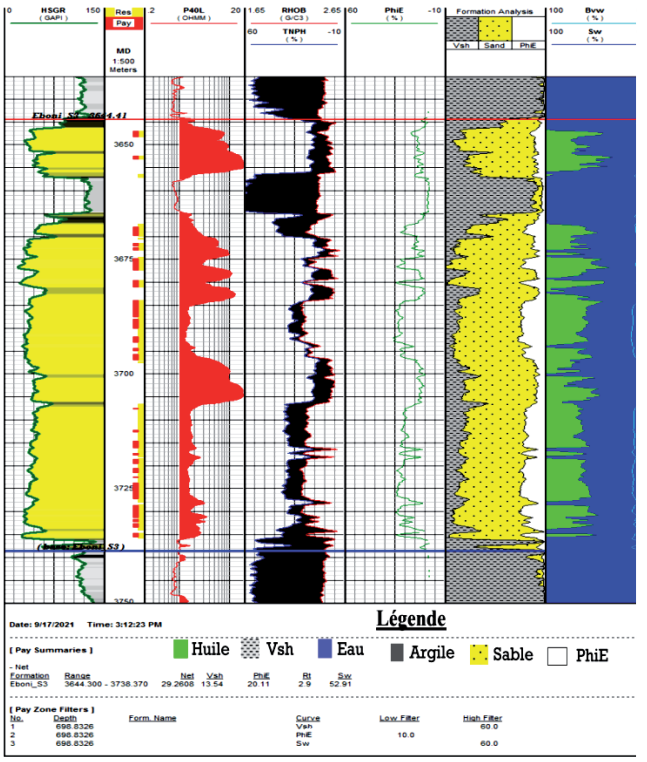

Figure 17. The litho-saturation plots of reservoir 3 of well 2
Рисунок 17. Графики литонасыщения пласта 3 скважины 2

Table 2. Petrophysical parameters of reservoir in well P1
Таблица 2. Петрофизические параметры пласта скважины P1

Reservoirs	Depth, m, TVD	Thickness, m	V_{sh}, %	PhiE, %	S_w, %	lithology	Natural fluids
R1	3340–3369	29.35	29.47	20.97	47.45	Sandy shale	Gas
R2	3508–3587	78.65	22.46	17.37	54.35	Sandy shale	Gas
R3	3644–3738	94.07	15.54	20.11	52.91	Sandy shale	Gas

density-neutron logs of the reservoirs selected (Figs. 15–17), this could indicate the presence of gas in these reservoirs. A variation in resistivity logs can show that the fluids of the formations crossed are more or less permeable and porous (sand-clay). In addition, the effective porosity logs (PhiE) obtained confirm the two hypotheses. Table 2 below shows the synthesis of the petrophysical parameters obtained after evaluation of reservoir 2.

The assessment of the hydrocarbon potential of the Cretaceous formations in the south of the Douala/Kribi-Campo basin was carried out using 3D seismic and well data analyses. Several hypotheses have been put forward to show the productivity of the basin. The seismic interpretation shows that the formations of the Lower Cretaceous (Aptian) and those of the Upper Cretaceous (Campanian) present a petroleum interest or potential reservoirs. Furthermore, the petrophysical evaluation of the two existing wells in the study area does not show a large enough number of potential reservoirs.

Considering the results obtained, it appears that, the sediments come mainly from the continental shelf coming from the East and were deposited on the seabed by a phenomenon of gradation forming channels. Previous wells made based on 2D seismic could not reach the targeted prospects. Analysis of two wells shows the presence of sand and shale banks at depths of over 3000 m. Furthermore, the Net/Pay ratio gives the exact proportion of hydrocarbons in these reservoirs. Thus, the Cretaceous formations, more specifically the Logbaba (Campanian) and Mundeck (Albian-Aptian) formations can be considered as areas of interest from the oil/gas point of view.

Conclusions

This research presents an integrated study of well log analysis and 3D seismic analysis for hydrocarbon reservoir an the nature of fluids content investigation in the southern part of DKC oil field. The geophysical investigation shows that the southern part of the DKC basin exhibit a hydrocabure potential manifestation. The 3D seismic gives potential areas of petroleum accumulation on the amplitude maps. The nature of fluids consists of gas, gas/oil and water. Five reservoirs have been identified in well P1 and three in well P2. The reservoirs lithology encounter are mostly the sand and sandy clay. The presence of petroleum interest is observed to the South and East of the Aptian-Campanian Formations; moreover, the logging data confirms the hypothesis that the sandy reservoirs targeted by the two wells do not have a high hydrocarbon potential. This work can serve for the future petroleum field reservoir in the DKC basin and will avoid the wrong position of future wells.

REFERENCES

1. Pletsch T., Erbacher J., Holbourn A. E., Kuhnt W., Moullade M., Oboh-Ikuenobede F. E., Söding E., Wagner T. 2001, Cretaceous separation of Africa and South America: the view from the West African margin (ODP leg 159). *Journal of South American Earth Sciences*, vol. 14, issue 2, pp. 147–174. https://doi.org/10.1016/s0895-9811(01)00020-7

2. Tohver E., D'Agrella-Filho M. S., Trindade R. I. F. 2006, Paleomagnetic record of Africa and South America for the 1200–500 Ma interval, and evaluation of Rodinia and Gondwana assemblies. *Precambrian Research*, vol. 147, issue 3–4, pp. 193–222. https://doi.org/10.1016/j.precamres.2006.01.015

3. Brownfield M. E., Charpentier R. R. 2006, Geology and Total Petroleum Systems of the West-Central Coastal Province (7203), West Africa. Reston, Virginia: U. S. Geological Survey Bulletin 2207-B, 52 p.

4. SNH. 2005, Synthèse sur le Bassin du Rio Del Rey et sur le bassin de Douala/Kribi-Campo. Rapport interne 14. SNH, 2019. Bilan de prospective du bassin de Douala Kribi Campo, 14 p.

5. Vail P. R., Todd R. G., Sangree J. B. 1977, Seismic stratigraphy and global changes of sea level, Part 5: chronostratigraphic significance of seismic reflections. Seismic Stratigraphy – Applications to Hydrocarbon Exploration. C. E. Payton (ed.). Tulsa, Oklahoma: American Association of Petroleum Geologists, vol. 26, pp. 99–116. https://doi.org/10.1306/M26490C7

6. Sloss L. L. 1963, Sequences in the cratonic interior of North America. *Geological Society of America Bulletin*, vol. 74, no. 2, pp. 93–114. https://doi.org/10.1130/0016-7606(1963)74[93:SITCIO]2.0.CO;2

7. Obimma K. J., Obiora D. N., Oha A. I., Ibuot J. C., Yakubu J. A., 2021. Seismic and petrophysical characterization of reservoirs in Kjoe field, on-Shore Niger Delta, Nigeria. *Petroleum and Coal*, vol. 63, issue 1, pp. 50–62.

8. Posamentier H. W., Allen G. P., James D. P., Tesson M. 1992, Forced regressions in a sequence stratigraphic framework: concepts, examples, and exploration significance. *American Association of Petroleum Geologists Bulletin*, vol. 76, pp. 1687–1709.

9. Asquith G. B., Gibson C. R. 1982, Basic Well Log Analysis for Geologists. Tulsa, Oklahoma: American Association of Petroleum Geologists, 216 p.

10. Plint A. G., Nummedal D. 2000, The falling stage systems tract: recognition and importance in sequence stratigraphic analysis. Sedimentary Responses to Forced Regressions. D. Hunt, and R. L. Gawthorpe (eds). London: Geological Society, London, Special Publications, vol. 172, pp. 1–17. https://doi.org/10.1144/GSL.SP.2000.172.01.01

11. Payton C. E. 1977, Seismic Stratigraphy – applications to Hydrocarbon Exploration. Tulsa, Oklahoma: American Association of Petroleum Geologists, vol. 26. 516 p.

12. Radwan A. A., Abdelwahhab M. A., Nabawy B. S., Mahfouz K. H., Ahmed M. S. 2022, Facies analysis-constrained geophysical 3D-static reservoir modeling of Cenomanian units in the Aghar Oilfield (Western Desert, Egypt): insights into paleoenvironment and petroleum geology of fluviomarine systems. *Marine and Petroleum Geology*, vol. 136, pp. 105–436. https://doi.org/10.1016/j.marpetgeo.2021.105436

13. Mitchum R. M., Vail P. R., Thompson S. 1977, Seismic stratigraphy and global changes of sea level, Part 2: the depositional sequence as the basic unit for stratigraphic analysis. Seismic Stratigraphy – Applications to Hydrocarbon Exploration. C. E. Payton (ed.). Tulsa, Oklahoma: American Association of Petroleum Geologists, memoir 26, pp. 53–62. https://doi.org/10.1306/M26490C4

14. Schlumberger. 1998, Log Interpretation Charts. Sugar Land, Texas: Schlumberger Wireline and Testing, 176 p.

15. Doust H., Omatsola E. 1990, Niger Delta. Divergent/Passive Margin Basins. J. D. Edwards, P. A. Santogrossi (Eds). Tulsa, Oklahoma: American Association of Petroleum Geologists, vol. 48, pp. 201–238. https://doi.org/10.1306/M48508C4

16. Miall A. D. 1992, Exxon global cycle chart: an event for every occasion? *Geology*, vol. 20, no. 9, pp. 787–790. https://doi.org/10.1130/0091-7613(1992)020<0787:EGCCAE>2.3.CO;2

17. Edwards J. D., Santogrossi P. A. 1990, Summary and conclusions. Divergent/Passive Margin Basins. J. D. Edwards, P. A. Santogrossi (Eds). Tulsa, Oklahoma: American Association of Petroleum Geologists, vol. 48, pp. 239–248. https://doi.org/10.1306/M48508C5

18. Abdelmaksoud A., Radwan A. A. 2022, Integrating 3D seismic interpretation, well log analysis and static modelling for characterizing the Late Miocene reservoir, Ngatoro area, New Zealand. *Geomechanics and Geophysics for Geo-Energy and Geo-Resources*, vol. 8, issue 2, pp. 1–31. http://dx.doi.org/10.1007/s40948-022-00364-8

19. Abdelwahhab M. A., Radwan A. A., Mahmoud H., Mansour A. 2022, Geophysical 3D-static reservoir and basin modeling of a Jurassic estuarine system (JG-Oilfield, Abu Gharadig basin, Egypt). *Journal of Asian Earth Sciences*, vol. 225, article number 105067. https://doi.org/10.1016/j.jseaes.2021.105067

20. Mellere D. 1994, Sequential development of an estuarine valley fill: the Twowells Tongue of the Dakota Sandstone, Acoma Basin, New Mexico. *Journal of Sedimentary Research*, vol. B64(4), pp. 500–515.

21. Reyre D. 1964, Histoire géologique du bassin de Douala Elf Serepca D.E/S.GL.C. Note interne.

22. Regnoult J. M. 1986, Synthèse Géologique du Cameroun. Yaoundé: Ministère des Mines et de l'nergie, 119 p.

23. Nguene F. R., Tamfu S., Loule J. P., Ngassa C. 1992, Paleoenvironments of the Douala and Kribi-Campo sub-basins in Cameroon, West Africa. Géologie Africaine. Bulletin du Centre de Recherche Exploration-Production Elf-Aquitaine. R. Curnelle (ed.), Memoire 13, pp. 129–139.

24. Tamfu S. F., Batupe M., Pauken R. J., Boatwright D. C. 1995, Geological setting, stratigraphy and hydrocarbon habitat of the Douala Basin, Cameroon. *The American Association of Petroleum Geologists Bulletin*, vol. 79, no. 13, pp. 1–95.

25. Ntamak-Nida M. J., Bourquin S., Makong J.-C., Baudin F., Mpesse J. E., Ngouem C. I., Komguem P. B., Abolo G. M. 2010, Sedimentology and sequence stratigraphy from outcrops of the Kribi-Campo Sub-basin: lower Mundeck formation (lower cretaceous, southern Cameroon). *Journal of African Earth Sciences*, vol. 58, issue 1, pp. 1–18. https://doi.org/10.1016/j.jafrearsci.2010.01.004

26. Giresse P. 1990, Esquisse géologique de l'Afrique centrale occidentale. Paysages quaternaires de l'Afrique centrale occidentale. Paris: ORSTOM. URL: http://horizon.documentation.ird.fr, pp. 15–19.

27. Lawrence S. R., Munday S., Bray R. 2002, Regional Geology and Geophysics of the Eastern Gulf of Guinea (Niger Delta to Rio Muni). *The Leading Edge*, vol. 21, issue 21, pp. 1112–1117. https://doi.org/10.1190/1.1523752

28. Galloway W. E. 1989, Genetic stratigraphic sequences in basin analysis I: architecture and genesis of flooding-surface bounded depositional units. *The American Association of Petroleum Geologists Bulletin*, vol. 73, issue 2, pp. 125–142. https://doi.org/10.1306/703C9AF5-1707-11D7-8645000102C1865D

29. Dumort J. D. 1968, Notice Explicative sur la feuille Douala-Ouest. Carte Geologique de reconnaissance (1/500 000). Yaoundé, Cameroon: Direction des Mines et de la Geologie du Cameroun, 69 p.

30. Meyers J. B., Rosendahl B. R., Groschel-Becker H., Austin Jr. J. A., Rona P. A. 1996, Deep penetrating MCS imaging of the rift-to drift transition, offshore Douala and North Gabon basins, West Africa. *Marine and Petroleum Geology*, vol.13, issue 7, pp. 791–835. https://doi.org/10.1016/0264-8172(96)00030-X

31. ECL. 2001, An integrated study of structural development, source rock maturity and hydrocarbon generation in the Douala/Kribi-Campo basin, Republic of Cameroon. Rapport interne SNH. 185 p.

32. Logar J. F. 1983, WEC Afrique de l'ouest: Well Evaluation conference, published by Schlumberger, sl., pp. 1–69.

33. Robertson C. G. G. 2015, Petroleum Geological Evaluation: Niger Delta to the Congo Fan. CGG Robertson Multiclient. Report No. AM086.

34. Campbell C. V. 1967, Lamina, Laminaset, Bed, and Bedset. *Sedimentology*, vol. 8, issue 1, pp. 7–26. https://doi.org/10.1111/j.1365-3091.1967.tb01301.x

35. Belmonte Y. C. 1966, Stratigraphie du bassin sedimentaire du Cameroun. Proceedings of 2nd West African Micropaleontology Colloquium. Ibadan, pp. 65–77.
36. Salard-Chebodaeff M. 1977, Palynologie du bassin sédimentaire Littoral du Cameroun dans ses rapports avec la stratigraphie et la paléoécologie. Thèse de Doctorat d'Etat ès Sciences naturelles, 262 p.
37. Njike Ngaha P. R. 2004, Palynostratigraphie et Reconstitution des Paléoenvironnements du Crétacé de l'Est du bassin Sédimentaire de Douala (Cameroun). Thèse de Doctorat d'Etat. Yaoundé, Cameroon: Université de Yaoundé I, 258 p.
38. Abdel-Fattah M. I., Alrefaee H. A. 2014, Diacritical seismic signatures for complex geological structures: case studies from Shushan Basin (Egypt) and Arkoma Basin (USA). *International Journal of Geophysics*, vol. 2014, pp. 1–14. https://doi.org/10.1155/2014/876180
39. Howard R. E. 1991, Landmark Graphics Corporation. Method for attribute tracking in seismic data. Brevet American 5, pp. 56–66.
40. Serra O. 1979, Diagraphies Différés base de l'interprétation. Mémoire 1, Tome 1. Services techniques. Paris: Schlumberger, 631 p.
41. 1999, Mesozoic and Cenozoic Sequence Stratigraphy of European Basins. P. de Graciansky, J. Hardenbol, T. Jacquin, P. R. Vail (eds). Tulsa, Oklahoma: SEPM Special Publication, vol. 60, pp. 3–29. https://doi.org/10.2110/pec.98.02
42. Meunier M. 2011, Diagraphie di érée. IFP Training, 134 p.
43. Clavier C., Coates G., Dumanoir J. 1977, Theoretical and Experimental Bases for the Dual-Water Model for Interpretation of Shaly Sands. *Society of Petroleum Engineers Journal*, vol. 24, issue 2, pp. 153–168. https://doi.org/10.2118/6859-PA
44. Gay A., Lopez M., Cochonat P., Sermondadaz G. 2004, Polygonal faults-furrows system related to early stages of compaction-Upper Miocene to recent sediments of the Lower Congo Basin. *Basin Research*, vol. 16, issue 1, pp. 101–116. https://doi.org/10.1111/j.1365-2117.2003.00224.x

The article was received on November 25, 2023

УДК 550.839 http://doi.org/10.21440/2307-2091-2024-1-33-46

Гео-петрофизический анализ углеводородов в бассейне Дуала-Кампо, Камерун

Барежа ЙОМССИ ТИШУЕ[1*]
Валентина Михайловна УСОВА[2**]
Сикстус НТЕХ[1***]
Елена Михайловна КОТЕЛЬНИКОВА[2****]

[1]Университет Баменды, Баменда, Камерун
[2]Российский университет дружбы народов (РУДН), Москва, Россия

Аннотация

Актуальность работы. Анализ каротажа скважин и метод 3D-сейсморазведки объединяются для оценки характера флюидов и характеристик коллектора в бассейне Дуала-Кампо (ДК). Научные исследования, раскрывающие важные геологические и геофизические условия этого бассейна, отсутствуют.

Цель работы. Успешное исследование этих территорий возможно при условии правильной оценки стратиграфических и петрофизических свойств коллектора.

Методология исследования. Извлечение фациальных типов из сейсмических разрезов 3D является быстроразвивающейся дисциплиной, которая облегчает разработку моделей прогнозирования коллекторов. Поэтому была построена сейсмическая сетка размером 25 х 25 м, связанная с гамма-каротажем (GR), нейтронным каротажем (Nphi), каротажем удельного сопротивления, акустическим каротажем и каротажем плотности (RHOB).

Результаты и выводы. Результаты отражают осадочную среду и фацию, пористо-проницаемые глинистые отложения, глинистость, пористость, насыщенность и природу флюидов в коллекторе. Петрофизические оценки указывают на потенциальные залежи нефти, преимущественно песчано-глинистые с объемом 3,81–29,47 %, пористостью 17,37–27,85 % и водонасыщенностью 47,74–56,02 %. В пласте присутствуют нефть, газ и вода. Это исследование будет способствовать разведке углеводородов (УВ) в бассейне округа Колумбия за счет принятия стратегий, в которых сейсмическая стратиграфия в сочетании с данными скважин будет наиболее вероятным средством определения целей бурения для более независимых операторов. Результаты этого исследования послужат будущим старателям на соседних месторождениях нефти и газа в районе нашего исследования. Были достигнуты значительные успехи для обеспечения будущих успехов в разведке.

***Ключевые слова*:** 3D-сейсморазведка, пласт, каротаж, петрофизические параметры, ДК.

ЛИТЕРАТУРА

1. Pletsch T., Erbacher J., Holbourn A. E., Kuhnt W., Moullade M., Oboh-Ikuenobede F. E., Söding E., Wagner T. Cretaceous separation of Africa and South America: the view from the West African margin (ODP leg 159) // Journal of South American Earth Sciences. 2001. Vol. 14. Issue 2. P. 147–174. https://doi.org/10.1016/s0895-9811(01)00020-7
2. Tohver E., D'Agrella-Filho M. S., Trindade R. I. F. Paleomagnetic record of Africa and South America for the 1200–500 Ma interval, and evaluation of Rodinia and Gondwana assemblies // Precambrian Research. 2006. Vol. 147. Issue 3–4. P. 193–222. https://doi.org/10.1016/j.precamres.2006.01.015
3. Brownfield M. E., Charpentier R. R. Geology and Total Petroleum Systems of the West-Central Coastal Province (7203), West Africa. Reston, Virginia: U.S. Geological Survey Bulletin 2207-B, 2006. 52 p.
4. SNH. Synthèse sur le Bassin du Rio Del Rey et sur le bassin de Douala/Kribi-Campo. Rapport interne 14. SNH, 2019. Bilan de prospective du bassin de Douala Kribi Campo, 2005. 14 p.
5. Vail P. R., Todd R. G., Sangree J. B. Seismic stratigraphy and global changes of sea level, Part 5: chronostratigraphic significance of seismic reflections. Seismic Stratigraphy – Applications to Hydrocarbon Exploration. C. E. Payton (ed.). Tulsa, Oklahoma: American Association of Petroleum Geologists, 1977, vol. 26, pp. 99–116. https://doi.org/10.1306/M26490C7
6. Sloss L. L. Sequences in the cratonic interior of North America // Geological Society of America Bulletin. 1963. Vol. 74. No. 2. P. 93–114. https://doi.org/10.1130/0016-7606(1963)74[93:SITCIO]2.0.CO;2
7. Obimma K. J., Obiora D. N., Oha A. I., Ibuot J. C., Yakubu J. A., Seismic and petrophysical characterization of reservoirs in Kjoe field, on-Shore Niger Delta, Nigeria // Petroleum and Coal. 2021. Vol. 63. Issue 1. P. 50–62.
8. Posamentier H. W., Allen G. P., James D. P., Tesson M. Forced regressions in a sequence stratigraphic framework: concepts, examples, and exploration significance // American Association of Petroleum Geologists Bulletin. 1992. Vol. 76. P. 1687–1709.

✉youmssi@mail.ru
** usova-vm@rudn.ru
https://orcid.org/0000-0002-0023-5913
***ntehsixtus@gmail.com
****kotelnikova-em@rudn.ru
https://orcid.org/0000-0001-8909-8953

9. Asquith G. B., Gibson C. R. Basic Well Log Analysis for Geologists. Tulsa, Oklahoma: American Association of Petroleum Geologists, 1982. 216 p.
10. Plint A. G. Nummedal D. The falling stage systems tract: recognition and importance in sequence stratigraphic analysis. Sedimentary Responses to Forced Regressions. Ed. by D. Hunt, R. L. Gawthorpe. London: Geological Society, London, Special Publications, 2000. Vol. 172. P. 1–17. https://doi.org/10.1144/GSL.SP.2000.172.01.01
11. Payton C. E. Seismic Stratigraphy – applications to Hydrocarbon Exploration. Tulsa, Oklahoma: American Association of Petroleum Geologists, 1977. Vol. 26. 516 p.
12. Radwan A. A., Abdelwahhab M. A., Nabawy B. S., Mahfouz K. H., Ahmed M. S. Facies analysis-constrained geophysical 3D-static reservoir modeling of Cenomanian units in the Aghar Oilfield (Western Desert, Egypt): insights into paleoenvironment and petroleum geology of fluviomarine systems // Marine and Petroleum Geology. 2022. Vol. 136. P. 105–436. https://doi.org/10.1016/j.marpetgeo.2021.105436
13. Mitchum R. M., Vail P. R., Thompson S. Seismic stratigraphy and global changes of sea level, Part 2: the depositional sequence as the basic unit for stratigraphic analysis. Seismic Stratigraphy – Applications to Hydrocarbon Exploration. Ed. by C. E. Payton. Tulsa, Oklahoma: American Association of Petroleum Geologists, 1977. Vol. 26. P. 53–62. https://doi.org/10.1306/M26490C4
14. Schlumberger. Log Interpretation Charts. Sugar Land, Texas: Schlumberger Wireline and Testing, 1998. 176 p.
15. Doust H., Omatsola E. Niger Delta. Divergent/Passive Margin Basins. Ed. by J. D. Edwards, P. A. Santogrossi. Tulsa, Oklahoma: American Association of Petroleum Geologists, 1990. Vol. 48. P. 201–238. https://doi.org/10.1306/M48508C4
16. Miall A. D. Exxon global cycle chart: an event for every occasion? // Geology. 1992. Vol. 20. No. 9. P. 787–790. https://doi.org/10.1130/0091-7613(1992)020<0787:EGCCAE>2.3.CO;2
17. Edwards J. D., Santogrossi P. A. Summary and conclusions. Divergent/Passive Margin Basins. Ed. by J. D. Edwards, P. A. Santogrossi. Tulsa, Oklahoma: American Association of Petroleum Geologists, 1990. Vol. 48. P. 239–248. https://doi.org/10.1306/M48508C5
18. Abdelmaksoud A., Radwan A. A. Integrating 3D seismic interpretation, well log analysis and static modelling for characterizing the Late Miocene reservoir, Ngatoro area, New Zealand // Geomechanics and Geophysics for Geo-Energy and Geo-Resources. 2022. Vol. 8. Issue 2. P. 1–31. http://dx.doi.org/10.1007/s40948-022-00364-8
19. Abdelwahhab M. A., Radwan A. A., Mahmoud H., Mansour A. Geophysical 3D-static reservoir and basin modeling of a Jurassic estuarine system (JG-Oilfield, Abu Gharadig basin, Egypt) // Journal of Asian Earth Sciences. 2022. Vol. 225. Article number 105067. https://doi.org/10.1016/j.jseaes.2021.105067
20. Mellere D. Sequential development of an estuarine valley fill: the Twowells Tongue of the Dakota Sandstone, Acoma Basin, New Mexico // Journal of Sedimentary Research. 1994. Vol. B64(4). P. 500–515.
21. Reyre D. Histoire géologique du bassin de Douala Elf Serepca D.E/S.GL.C. Note interne, 1964.
22. Regnoult J. M. Synthèse Géologique du Cameroun. Yaoundé: Ministère des Mines et de l'nergie, 1986. 119 p.
23. Nguene F. R., Tamfu S., Loule J. P., Ngassa C. Paleoenvironments of the Douala and Kribi-Campo sub-basins in Cameroon, West Africa. Géologie Africaine. Bulletin du Centre de Recherche Exploration-Production Elf-Aquitaine. Ed. by R. Curnelle. 1992. Vol. 13. P. 129–139.
24. Tamfu S. F., Batupe M., Pauken R. J., Boatwright D. C. Geological setting, stratigraphy and hydrocarbon habitat of the Douala Basin, Cameroon // The American Association of Petroleum Geologists Bulletin. 1995. Vol. 79. No. 13. P. 1–95.
25. Ntamak-Nida M. J., Bourquin S., Makong J.-C., Baudin F., Mpesse J. E., Ngouem C. I., Komguem P. B., Abolo G. M. Sedimentology and sequence stratigraphy from outcrops of the Kribi-Campo Sub-basin: lower Mundeck formation (lower cretaceous, southern Cameroon) // Journal of African Earth Sciences. 2010. Vol. 58. Issue 1. P. 1–18. https://doi.org/10.1016/j.jafrearsci.2010.01.004
26. Giresse P. Esquisse géologique de l'Afrique centrale occidentale. Paysages quaternaires de l'Afrique centrale occidentale. Paris: ORSTOM, 1990. URL: http://horizon.documentation.ird.fr, pp. 15–19.
27. Lawrence S. R., Munday S., Bray R. Regional Geology and Geophysics of the Eastern Gulf of Guinea (Niger Delta to Rio Muni) // The Leading Edge. 2002. Vol. 21. Issue 21. P. 1112–1117. https://doi.org/10.1190/1.1523752
28. Galloway W. E. Genetic stratigraphic sequences in basin analysis I: architecture and genesis of flooding-surface bounded depositional units // The American Association of Petroleum Geologists Bulletin. 1989. Vol. 73. Issue 2. P. 125–142. https://doi.org/10.1306/703C9AF5-1707-11D7-8645000102C1865D
29. Dumort J. D. Notice Explicative sur la feuille Douala-Ouest. Carte Geologique de reconnaissance (1/500 000). Yaoundé, Cameroon: Direction des Mines et de la Geologie du Cameroun, 1968. 69 p.
30. Meyers J. B., Rosendahl B. R., Groschel-Becker H., Austin Jr. J. A., Rona P. A. Deep penetrating MCS imaging of the rift-to drift transition, offshore Douala and North Gabon basins, West Africa // Marine and Petroleum Geology. 1996. Vol. 13. Issue 7. P. 791–835. https://doi.org/10.1016/0264-8172(96)00030-X
31. ECL. An integrated study of structural development, source rock maturity and hydrocarbon generation in the Douala/Kribi-Campo basin, Republic of Cameroon. Rapport interne SNH, 2001. 185 p.
32. Logar J. F. WEC Afrique de l'ouest: Well Evaluation conference, published by Schlumberger, sl., 1983. P. 1–69.
33. Robertson C. G. G. Petroleum Geological Evaluation: Niger Delta to the Congo Fan. CGG Robertson Multiclient. Report No. AM086, 2015.
34. Campbell C. V. Lamina, Laminaset, Bed, and Bedset // Sedimentology. 1967. Vol. 8. Issue 1. P. 7–26. https://doi.org/10.1111/j.1365-3091.1967.tb01301.x
35. Belmonte Y. C. Stratigraphie du bassin sedimentaire du Cameroun. Proceedings of 2nd West African Micropaleontology Colloquium. Ibadan, 1966. P. 65–77.
36. Salard-Chebodaeff M. Palynologie du bassin sédimentaire Littoral du Cameroun dans ses rapports avec la stratigraphie et la paléoécologie. Thèse de Doctorat d'Etat ès Sciences naturelles, 1977. 262 p.
37. Njike Ngaha P. R. Palynostratigraphie et Reconstitution des Paléoenvironnements du Crétacé de l'Est du bassin Sédimentaire de Douala (Cameroun). Thèse de Doctorat d'Etat. Yaoundé, Cameroon: Université de Yaoundé I, 2004, 258 p.
38. Abdel-Fattah M. I., Alrefaee H. A. Diacritical seismic signatures for complex geological structures: case studies from Shushan Basin (Egypt) and Arkoma Basin (USA) // International Journal of Geophysics. 2014. Vol. 2014. P. 1–14. https://doi.org/10.1155/2014/876180
39. Howard R. E. Landmark Graphics Corporation. Method for attribute tracking in seismic data. Brevet American 5, 1991. P. 56–66.
40. Serra O. Diagraphies Différés base de l'interprétation. Mémoire 1, Tome 1. Services techniques. Paris: Schlumberger, 1979. 631 p.
41. Mesozoic and Cenozoic Sequence Stratigraphy of European Basins. Ed. by P. de Graciansky, J. Hardenbol, T. Jacquin, P. R. Vail. Tulsa, Oklahoma: SEPM Special Publication, 1999. Vol. 60, pp 3–29. https://doi.org/10.2110/pec.98.02
42. Meunier M. Diagraphie di érée. IFP Training, 2011. 134 p.
43. Clavier C., Coates G., Dumanoir J. Theoretical and Experimental Bases for the Dual-Water Model for Interpretation of Shaly Sands // Society of Petroleum Engineers Journal. 1977. Vol. 24. Issue 2. P. 153–168. https://doi.org/10.2118/6859-PA
44. Gay A., Lopez M., Cochonat P., Sermondadaz G. Polygonal faults-furrows system related to early stages of compaction-Upper Miocene to recent sediments of the Lower Congo Basin // Basin Research. 2004. Vol. 16. Issue 1. P. 101–116. https://doi.org/10.1111/j.1365-2117.2003.00224.x

Статья поступила в редакцию 25 ноября 2023 года